

Electron-phonon mass enhancement and lifetime at finite temperature

F. Marsiglio

*Neutron & Condensed Matter Science, AECL, Chalk River Laboratories, Chalk River, Ontario, Canada K0J 1J0;
Department of Physics & Astronomy, McMaster University, Hamilton, Ontario L8S 4M1;
and Canadian Institute for Advanced Research, McMaster University, Hamilton, Ontario L8S 4M1*

(Received 29 October 1996)

We reexamine the effect of the electron-phonon interaction on the electron mass enhancement and inverse lifetime as a function of temperature. We assign the values of the quasiparticle energy and inverse lifetime to the real and imaginary parts of the pole in the single-electron Green function, following Galitskii and Migdal. We find that for intermediate to strong coupling the electron mass enhancement grows monotonically with temperature and the electron inverse lifetime is almost independent of the electron-phonon coupling parameter. This result corrects the conventional wisdom that the mass enhancement has a maximum as a function of temperature, and that the inverse lifetime grows linearly with coupling constant, statements which remain true for weak coupling. In contrast, electron-impurity scattering leads to a decrease of the electron mass enhancement parameter. [S0163-1829(97)01212-5]

Historically, the single-electron Green function has played a very important role in our understanding of the impact of electron-phonon interactions on the properties of the electron.^{1,2} In particular, the real and imaginary parts of the pole in the single-electron Green function are normally identified with the quasiparticle energy and inverse lifetime, respectively. Such a correspondence is strictly meaningful only if certain conditions are met, for example, the quasiparticles are restricted to lie right on the Fermi surface.³ Nonetheless, very often the usefulness of the quasiparticle concept continues away from the Fermi surface, and indeed, under other conditions where, strictly speaking, the concept is no longer valid. One such ‘‘continuation’’ is to finite temperature. Thus, it is common practice to define an electron mass enhancement parameter and an inverse lifetime, for temperatures above the absolute zero,^{4,5} particularly in the electron-phonon problem. Here we reexamine the electron mass enhancement and inverse lifetime for nonzero temperature. The result is a somewhat different physical picture than is normally presented.

We begin with the standard Migdal approximation for the electron self-energy in the electron-phonon problem,⁵

$$\Sigma_{\text{ph}}(\omega + i\delta) = \int_0^\infty d\nu \alpha^2 F(\nu) \left\{ -2\pi i \left[N(\nu) + \frac{1}{2} \right] + \psi \left(\frac{1}{2} + i \frac{\nu - \omega}{2\pi T} \right) - \psi \left(\frac{1}{2} - i \frac{\nu + \omega}{2\pi T} \right) \right\}, \quad (1)$$

where T is the temperature and ω is a real frequency. The function $\alpha^2 F(\nu)$ is the electron-phonon spectral function, $N(\nu)$ is the Bose function, and $\psi(x)$ is the digamma function. Recall that Eq. (1) comes from the lowest order (albeit self-consistent) Feynman diagram; hence the standard disregard for vertex corrections is inherent in Eq. (1). Furthermore, because of the usual disparate phonon and electron energy scales, Fermi surface averaging over the electron-phonon matrix elements makes the self-energy isotropic. In addition particle-hole symmetry together with the large electron bandwidth cause the Fermi-level energy scale to disappear from the problem and the self-consistency requirement is redundant.⁶ As a result of these approximations the expression (1) is in closed form.

The quasiparticle has the energy and lifetime defined by the pole of the single-electron retarded Green function,¹ i.e., the zero of

$$G^{-1}(\mathbf{k}, \omega + i\delta) = \omega - \epsilon_k - \Sigma_{\text{ph}}(\omega + i\delta), \quad (2)$$

where ϵ_k is the electron dispersion in the absence of interactions and now the functions are analytically continued to the lower half plane. Defining the energy and inverse lifetime by the pole in the lower half plane,

$$\omega \equiv E_k - i\Gamma_k/2, \quad (3)$$

we obtain the two equations,

$$E_k = \epsilon_k + \int_0^\infty d\nu \alpha^2 F(\nu) \text{Re} \left\{ \psi \left(\frac{1}{2} + i \frac{\nu - E_k + i\Gamma_k/2}{2\pi T} \right) - \psi \left(\frac{1}{2} - i \frac{\nu + E_k - i\Gamma_k/2}{2\pi T} \right) \right\}, \quad (4)$$

$$\Gamma_k = 2 \int_0^\infty d\nu \alpha^2 F(\nu) \left\{ 2\pi \left[N(\nu) + \frac{1}{2} \right] - \text{Im} \left(\psi \left(\frac{1}{2} + i \frac{(\nu - E_k + i\Gamma_k/2)}{2\pi T} \right) \right) - \psi \left(\frac{1}{2} - i \frac{(\nu + E_k - i\Gamma_k/2)}{2\pi T} \right) \right\}. \quad (5)$$

Here E_k gives the (new) dispersion in the presence of interactions and Γ_k gives the inverse lifetime (also hereafter referred to as the electron scattering rate). These equations must be solved self-consistently to obtain the quasiparticle pole, i.e., energy and lifetime. The conventional procedure is, however, to assume that both E_k and Γ_k are small so that one can obtain closed expressions. These are^{5,4}

$$E_k \approx \epsilon_k / [1 + \lambda^*(T)], \quad (6)$$

$$\Gamma^*(T) \approx \frac{4\pi \int_0^\infty d\nu \alpha^2 F(\nu) [N(\nu) + f(\nu)]}{1 + \lambda^*(T)}, \quad (7)$$

where $f(\nu)$ is the Fermi function and

$$\lambda^*(T) \approx -\frac{1}{\pi T} \int_0^\infty d\nu \alpha^2 F(\nu) \text{Im}\psi' \left(\frac{1}{2} + i \frac{\nu}{2\pi T} \right). \quad (8)$$

The function $\lambda^*(T)$ is often referred to as the mass enhancement parameter because of the way it enters Eq. (6). Both this function and $\Gamma^*(T)$ are independent of momentum so the momentum label has been dropped. Note that at zero temperature, $\lambda^*(T)$ reduces to the well-known electron-phonon coupling constant, $\lambda \equiv 2 \int_0^\infty d\nu [\alpha^2 F(\nu)/\nu]$. These expressions are obtained by expanding the denominator in Eq. (2) about the origin (where the pole at the Fermi surface resides in the noninteracting limit). In fact, Eq. (8) comes from $\lambda^*(T) = -\partial \Sigma(\omega)/\partial \omega$, where the right-hand side is evaluated at $\omega=0$. Indeed, this expansion is often taken as a ‘‘definition’’ of the mass enhancement parameter. However, in the high temperature limit $\lambda^*(T) \propto 1/T^2$, and $\Gamma^*(T) \propto T$, as defined above. The latter result is in conflict with the assumption that $\Gamma^*(T)$ is small. Thus Eqs. (7),(8) may be a poor approximations for nonzero temperatures.

As stated above the correct procedure is to solve Eqs. (4),(5) self-consistently. Such a procedure defines a different dispersion relation given by E_k . The usual practice is to define an effective mass (at least at the Fermi energy) and hence a mass enhancement parameter. Clearly the definition for this purpose is

$$1 + \lambda(T) \equiv (\partial E_k / \partial \epsilon_k)^{-1}. \quad (9)$$

To investigate the consequences, we hereafter confine ourselves to the Fermi surface ($\epsilon_k=0$). Then inspection of Eq. (4) reveals that $E_k=0$ remains a solution. We find (the asterisks are dropped to differentiate these solutions from the previous approximate ones)

$$\lambda(T) = -\frac{1}{\pi T} \int_0^\infty d\nu \alpha^2 F(\nu) \text{Im}\psi' \left(\frac{1}{2} - \frac{\Gamma(T)}{4\pi T} + i \frac{\nu}{2\pi T} \right), \quad (10)$$

where now the scattering rate is given by

$$\Gamma(T) = 4\pi \int_0^\infty d\nu \alpha^2 F(\nu) \left\{ N(\nu) + \frac{1}{2} - \frac{1}{\pi} \text{Im}\psi' \left(\frac{1}{2} - \frac{\Gamma(T)}{4\pi T} + i \frac{\nu}{2\pi T} \right) \right\}. \quad (11)$$

Equation (11) must now be solved numerically, as the right-hand side is a function of $\Gamma(T)$. Once this equation is solved, the result can be used in Eq. (10) to obtain $\lambda(T)$. Note that the new definition of $\lambda(T)$, Eq. (10), is simply related to the derivative of the self-energy, *but evaluated at the single-particle pole, not on the real axis.*

For an Einstein spectrum, $\alpha^2 F(\nu) = (\lambda \omega_E/2) \delta(\nu - \omega_E)$, so that Eqs. (10,11) reduce to dimensionless form [with $\gamma \equiv \Gamma(T)/\omega_E$ and $t \equiv T/\omega_E$]:

$$\gamma(t) = 2\pi\lambda \left\{ N(1/t) + \frac{1}{2} - \frac{1}{\pi} \text{Im}\psi' \left(\frac{1}{2} - \frac{\gamma(t)}{4\pi t} + \frac{i}{2\pi t} \right) \right\} \quad (12)$$

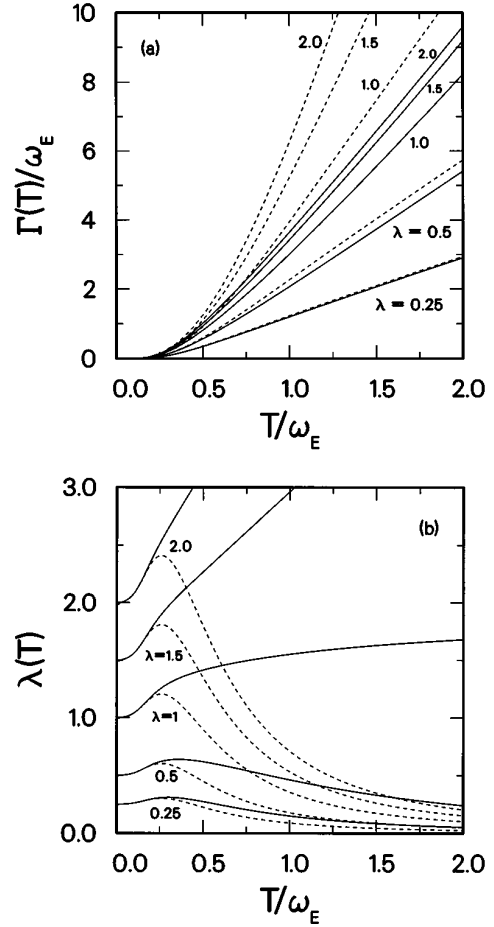


FIG. 1. (a) The normalized scattering rate vs the temperature for various coupling strengths. Solid curves are from Eq. (11) while dashed curves are obtained from the approximate expression Eq. (7). In all cases an Einstein spectrum was used (arbitrary frequency). (b) Electron mass enhancement parameter vs temperature for various coupling strengths. Solid curves are from Eq. (10) while dashed curves are obtained from the approximate expression Eq. (8).

and

$$\lambda(t) = -\frac{\lambda}{2\pi t} \text{Im}\psi' \left(\frac{1}{2} - \frac{\gamma(t)}{4\pi t} + \frac{i}{2\pi t} \right). \quad (13)$$

These results, along with their approximate counterparts [from Eq. (7,8)] are plotted in Fig. 1. Clearly, a precise determination of the pole [solid curves, from Eq. (11)] leads to a significantly lower scattering rate than that obtained using Eq. (7), particularly for coupling strengths that exceed unity. In fact, for high temperatures, the previous result led to the asymptotic behavior, $\Gamma(T) \approx 2\pi T\lambda$, while our result for high temperature is

$$\begin{aligned} \Gamma(T) &= 2\pi T\lambda \quad \text{for } \lambda < 1 \\ &= 2\pi T \quad \text{for } \lambda > 1. \end{aligned} \quad (14)$$

Interestingly, $\lambda=1$ demarcates weak from strong coupling behavior, as indicated by the electron scattering rate. In Fig. 1(b) $\lambda(T)$ is plotted for the same parameters. The high temperature behavior is remarkable, particularly for strong coupling. The mass enhancement $\lambda(T)$ *increases monotonically with temperature* for $\lambda > 1$. This is in contrast to the perturbative behavior (indicated by dashed curves) where a

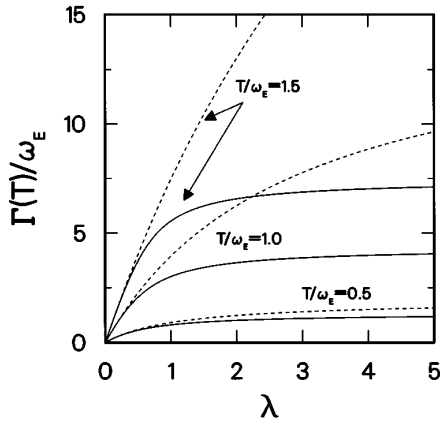


FIG. 2. The normalized scattering rate vs the coupling strength for various temperatures indicated. Note that the self-consistent results [solid curves, from Eq. (11)] saturate with increasing strength whereas the perturbative results vary as λ .

peak at low temperatures is followed by an asymptotic approach to zero for high temperature.⁴ In Fig. 2 we illustrate the scattering rate as a function of coupling strength for various temperatures. It is clear from this plot that the scattering rate saturates for strong coupling, whereas the perturbative expression Eq. (7) leads to a scattering rate which increases indefinitely with coupling strength. In particular, at very high temperatures (not shown) we obtain a kink in the result at $\lambda = 1$, as indicated by Eq. (14).

To understand these results, one must realize that the factor $1/[1+\lambda(T)]$ plays a dual role. On the one hand its inverse represents a mass enhancement, as signified by Eq. (6). In addition however, this factor gives the quasiparticle residue *at the pole*. As temperature increases it is plausible that the residue decreases since excited states are increasingly populated. Hence, while the scattering rate increases with increased coupling strength due to an increased interaction of the quasiparticle with the phonons, at the same time it has a tendency to decrease due to the decreasing weight of the quasiparticle. This also is consistent with the fact that at higher temperatures the energy dispersion should decrease, not increase, (since the original dispersion will become smeared), and hence $\lambda(T)$ should increase with temperature. This is apparently not true for weak coupling [see Fig. 1(b), the lower two sets of curves] indicative perhaps of insufficient (virtual) mixing of the electron wave function with the phonon wave functions.

Can these effects be measured? We suggest that very likely they cannot, as the following example shows. In many observables (and more directly in photoemission) the electron spectral function, $A(\mathbf{k}_F, \omega) \equiv -(1/\pi)G(\mathbf{k}_F, \omega + i\delta)$, plays an important role. We show this spectral function in Fig. 3 as a function of ω/ω_E , for various temperatures. The curves corresponding to the two lowest temperatures go off scale. The zero temperature curve has been understood in detail by Engelsberg and Schrieffer⁶ and others.⁷ Finite temperature smears the δ function (at the origin in this case) into an ever-broadening Lorentzian. This Lorentzian can be parametrized by a fitting procedure around $\omega = 0$:

$$A(\mathbf{k}_F, \omega) = \frac{1}{\pi} \frac{1}{1+\lambda^*(T)} \frac{\Gamma^*(T)/2}{\omega^2 + (\Gamma^*(T)/2)^2}, \quad (15)$$

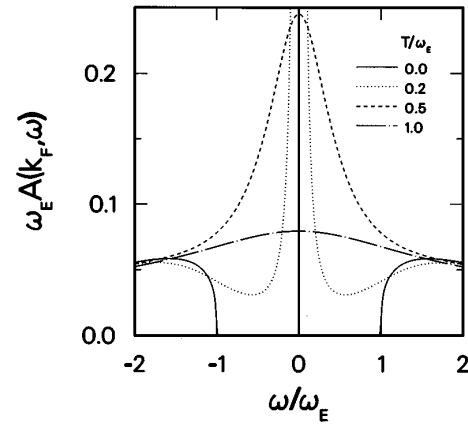


FIG. 3. The electron spectral function vs the frequency for $T/\omega_E = 0$ (solid), 0.2 (dotted), 0.5 (dashed), and 1.0 (dot-dashed). Here $\epsilon_k = 0$ and $\lambda = 1.5$.

where the parameters $\Gamma^*(T)$ and $\lambda^*(T)$ are given by Eqs. (7) and (8), i.e., the conventional scattering rate and mass enhancement. Thus, a determination of the area under the Lorentzian line shape (or the dispersion through several measurements) would yield a residue governed by the mass enhancement factor shown by the dashed curve (not the solid curve) in Fig. 1(b). In other words, the true dispersion and inverse lifetime, as defined by the pole of the single-electron Green function, are not useful for parametrizing the low energy spectral function for temperatures $T \gtrsim \omega_E$. On the other hand, the older definition (which, after all, is based on an expansion near $\omega = 0$) proves to be useful for this purpose. Therefore, even if sufficiently precise photoemission experiments could be performed, we would not observe the new behavior noted here. Similar remarks apply to cyclotron resonance⁸⁻¹¹ and specific heat⁴ measurements. These properties have a nonmonotonic temperature dependence similar to that given by $\lambda^*(T)$. The present work shows that it is incorrect to think of the specific heat at elevated temperatures, for example, as being primarily due to the specific heat of “dressed” quasiparticles.

Thus far we have attempted to extend the quasiparticle concept to finite temperature. The sharp increase of the electron scattering rate with temperature was seen to have a profound impact on the effective mass enhancement. This immediately suggests the following question: to what degree does ordinary impurity scattering (at zero temperature) result in similar effects? In the Born approximation the electron self-energy acquires a finite imaginary part:

$$\Sigma_{\text{imp}}(\omega + i\delta) = -(i/2\tau), \quad (16)$$

where $1/\tau$ is the electron-impurity scattering rate. The self-energy is now given by the sum of Eq. (16) and Eq. (1). The finite lifetime at zero temperature at the Fermi surface violates one of the fundamental requirements of a quasiparticle—that the inverse lifetime approach zero at the Fermi surface faster than the excitation energy itself³ (we also violated this requirement by going to finite temperature). Nonetheless, weak impurity scattering in the dilute limit is often looked upon as simply smearing the quasiparticle δ function into a somewhat broadened Lorentzian, and the quasiparticle characterization is often tacitly assumed. Confining our analysis

to an Einstein phonon spectrum and zero temperature, the mass enhancement and scattering rate from Eqs. (10),(11) become

$$\lambda(1/\tau) = \frac{\lambda}{1 + [\Gamma(1/\tau)/2\omega_E]^2}, \quad (17)$$

$$\Gamma(1/\tau)/2\omega_E = (1/\tau/2\omega_E) - \lambda \tan^{-1}[\Gamma(1/\tau)/2\omega_E]. \quad (18)$$

For weak impurity scattering ($1/\tau \ll \omega_E$) we recover conventional results: the quasiparticle scattering rate is *decreased* by the factor $1/[1 + \lambda]$, and to the first order the mass enhancement factor is unaffected by the impurity scattering. Numerical solutions to Eqs. (17),(18) are shown in Fig. 4 for various coupling strengths. *Contrary to the effect of finite temperature*, impurity scattering *increases* the scattering rate beyond the conventional result (dashed curves) and the mass enhancement factor is *suppressed*. Again, inspection of the spectral function reveals that the low energy peak is better characterized by the conventional result, i.e., a renormalized scattering rate, $\Gamma^*(1/\tau) = 1/[\tau(1 + \lambda)]$ with $\lambda^*(1/\tau) = \lambda$, rather than by the solutions of Eqs. (17),(18). Physically, the single-electron Green function becomes dominated by the impurity scattering as the scattering rate greatly exceeds the phonon frequency, so that the Green function can be characterized to a high accuracy by a single pole in the lower half plane.

In summary we have obtained self-consistent solutions for the simple poles in the electron Green function with phonon and impurity interactions, at finite temperature. Poles at the Fermi surface remain at the Fermi surface but acquire non-zero imaginary parts in the lower half plane. They are characterized by an effective mass and an effective scattering rate. The self-consistency requirement changes the temperature and impurity scattering rate significantly from that obtained in the conventional perturbative approach. Nonetheless, it remains difficult to probe this behavior experimentally, as most observables are more sensitive to the properties of the Green function on the real axis, not at the true quasiparticle pole. Electron-impurity scattering results in contrasting behavior; as the impurity scattering rate increases, the phonons become ineffectual, and the electron acquires a characteristic mass and lifetime that are independent of the electron-phonon interaction.

Perhaps the most significant impact of this work is a different view of quasiparticle excitations in regimes where, strictly speaking, the quasiparticle picture should not apply, e.g., at finite temperature. Figure 1(b), for example, shows that the mass enhancement at the pole agrees with the mass enhancement defined on the real axis [i.e., through Eq. (8) for $T/\omega_E \lesssim 0.2$]. For temperatures below this value the real

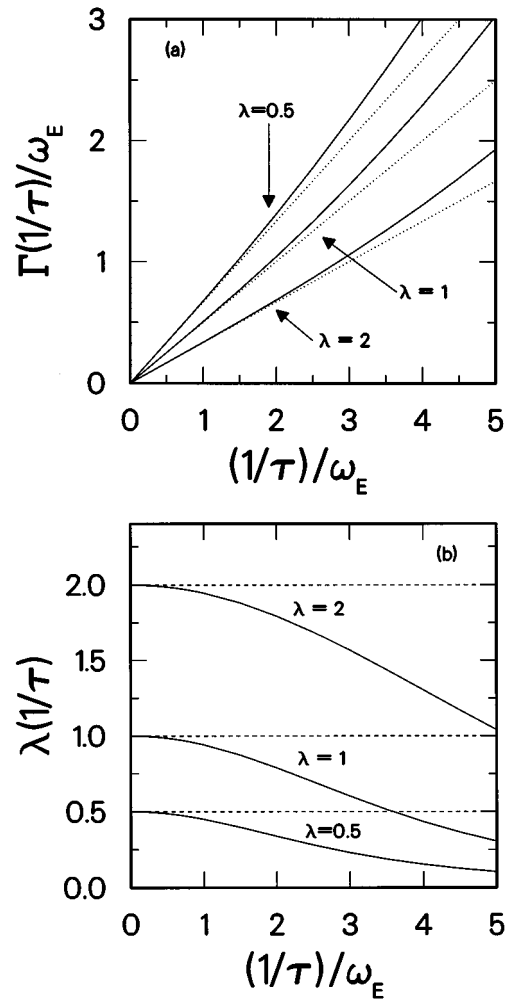


FIG. 4. (a) The normalized scattering rate vs the normalized impurity scattering rate for various coupling strengths, as indicated. The self-consistent results [solid curves, from Eq. (18)] are slightly higher than the conventional ones (dashed curves). (b) The mass enhancement parameter vs the normalized impurity scattering rate as in (a).

and imaginary parts of the quasiparticle pole are useful for parametrizing the spectral function, for example. For temperatures above this value, however, they are no longer useful, though they remain the energy and inverse lifetime of the quasiparticle. It then becomes clear that a description of the specific heat, for example, in terms of quasiparticles, is no longer meaningful for these elevated temperatures.

This research was partially supported by the Natural Sciences and Engineering Research Council (NSERC) of Canada and the Canadian Institute for Advanced Research (CIAR).

¹V.M. Galitskii and A.B. Migdal, Zh. Éksp. Teor. Fiz. **34**, 139 (1958) [Sov. Phys. JETP **7**, 96 (1958)].

²A.B. Migdal, Zh. Éksp. Teor. Fiz. **34**, 1438 (1958) [Sov. Phys. JETP **7**, 996 (1958)]; *Theory of Finite Fermi Systems and Applications to Atomic Nuclei* (Wiley, New York, 1967).

³P. Nozières, *Theory of Interacting Fermi Systems* (Benjamin, New York, 1964).

⁴G. Grimvall, *The Electron-Phonon Interaction in Metals* (North-Holland, New York, 1981).

⁵P.B. Allen and B. Mitrović, in *Solid State Physics: Advances in Research and Applications*, edited by H. Ehrenreich, F. Seitz, and D. Turnbull (Academic, New York, 1982), Vol. 37, p. 1.

⁶S. Engelsberg and J.R. Schrieffer, Phys. Rev. **131**, 993 (1963).

⁷K. Shimojima and H. Ichimura, Prog. Theor. Phys. **43**, 925 (1970).

⁸P. Goy and B. Castaing, Phys. Rev. B **7**, 4409 (1973).

⁹P.B. Allen, Phys. Rev. B **11**, 2693 (1975).

¹⁰P. Goy and B. Castaing, Phys. Rev. B **11**, 2696 (1975).

¹¹H. Scher and T. Holstein, Phys. Rev. **148**, 598 (1966).